molecular pharmaceutics

Article

pubs.acs.org/molecularpharmaceutics

Inhibiting Metastatic Breast Cancer Cell Migration via the Synergy of Targeted, pH-triggered siRNA Delivery and Chemokine Axis Blockade

Peng Guo,[†,‡,§] Jin-Oh You,[∥] Jiang Yang,[‡,§] Di Jia,[‡,§] Marsha A. Moses,[‡,§] and Debra T. Auguste*[,†,‡,§]

[†]Department of Biomedical Engineering, The City College of New York, 160 Convent Avenue, New York, New York 10031, United States

[‡]Vascular Biology Program, Boston Children's Hospital, 300 Longwood Avenue, Boston, Massachusetts 02115, United States

[§]Department of Surgery, Harvard Medical School, 25 Shattuck Street, Boston, Massachusetts 02115, United States

[∥]Department of Industrial Chemical Engineering, Chungbuk National University, Cheongju, 361-763, Republic of Korea

Supporting Information

ABSTRACT: Because breast cancer patient survival inversely correlates with metastasis, we engineered vehicles to inhibit both the C-X-C chemokine receptor type 4 (CXCR4) and lipocalin-2 (Lcn2) mediated migratory pathways. pH-responsive liposomes were designed to protect and trigger the release of Lcn2 siRNA. Liposomes were modified with anti-CXCR4 antibodies to target metastatic breast cancer (MBC) cells and block migration along the CXCR4-CXCL12 axis. This synergistic approach—coupling the CXCR4 axis blockade with Lcn2 silencing—significantly reduced migration in triple-negative human breast cancer cells (88% for MDA-MB-436 and 92% for MDA-MB-231). The results suggested that drug delivery vehicles engineered to attack multiple migratory pathways may effectively slow progression of MBC.

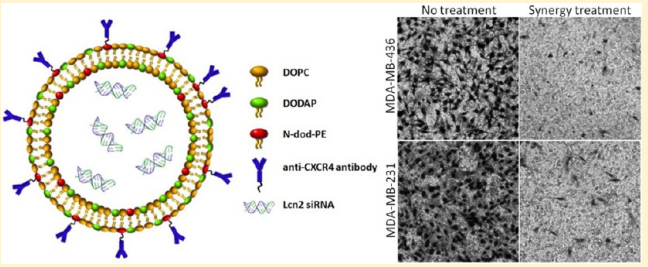

KEYWORDS: *CXCR4, liposome, siRNA, breast cancer, lipocalin-2, migration*

INTRODUCTION

Metastatic breast cancer (MBC) is the second leading cause of cancer-related fatality in women, accounting for more than 40,000 deaths each year.[1] MBC has a five-year relative survival rate of 23% compared with 99% for patients with nonmetastatic breast cancer.[1] These statistics suggest an urgent and significant need for developing novel and efficient therapeutics for the treatment of MBC.

A principal challenge in MBC treatment is to determine how to block MBC cell migration.[2] While many cancer therapies focus on cytotoxicity and targeting, few address migration, which inversely correlates with patient survival.[3] Ideally, an effective drug delivery strategy would possess multiple functions, including targeting, triggering delivery, and efficiently reducing MBC cell migration.

Although human epidermal growth factor receptor 2 (HER2) targeted therapeutics (trastuzumab,[4] lapatinib,[5] and neratinib[6]) have significantly improved the HER2 positive breast cancer prognostic outcome, HER2+ breast cancers comprise only approximately 20−25% of all breast cancers.[7] A variety of other receptors (e.g., transferrin receptor and epidermal growth factor receptor) are under intense investigation for targeting breast tumors;[8,9] their application is hindered by their expression on a number of normal tissues. An effective therapeutic target would have differential expression in breast cancer and normal tissues and be broadly identified on a range of breast cancers.

C-X-C chemokine receptor type 4 (CXCR4 or CD184) has been investigated extensively due to its potential role in metastasis.[10] CXCR4 is a G protein-coupled receptor that plays an important role in chemosensory transduction mechanisms in leukocytes and hematopoietic stem cells. It regulates cell migration along chemokine gradients, toward stromal derived factor 1 (SDF1 or CXCL12).[11] When CXCR4 is stimulated by its ligand SDF-1, CXCR4 couples with Gi family proteins and activates a number of signaling pathways involved in a variety of biological responses.[12] For example, CXCR4 ligand binding can lead to activation of PI3K and Rho family gtpases involved in the regulation of chemotaxis and survival.[12] Each of these molecules plays a primary role in MBC. CXCR4's role in cancer metastasis is confirmed by CXCR4 silencing and inhibition.[10]

In addition to receptor inhibition, we hypothesized that silencing of lipocalin-2 (Lcn2) at the same time would synergistically hinder cell migration. Lcn2, also referred to as neutrophil gelatinase-associated lipocalin (NGAL), is a secreted protein that is a member of the lipocalin protein superfamily. Increased Lcn2 levels have been reported in a variety of human epithelial cancers, including breast, ovarian, colon, pancreatic, and thyroid.[13] In breast cancer, high Lcn2 levels were associated with poor patient prognosis and advanced cancer status. Lcn2 is recognized as an independent prognostic marker

Received: August 7, 2013
Revised: January 22, 2014
Accepted: January 27, 2014
Published: January 27, 2014

for decreased survival.[14] We have previously shown that Lcn2 induced the epithelial to mesenchymal transition (EMT) in breast cancer cells and the knockdown of Lcn2 decreased breast cancer cell migration and invasion.[15] Consistent with our findings, deficiency of Lcn2 reduced tumor growth and metastasis in a transgenic mouse model of breast cancer.[16] For these reasons, we chose Lcn2 as a second target to inhibit metastasis.

Small interfering RNA (siRNA) is able to induce the destruction of specific mRNA sequences, altering the behavior of diseased cells. siRNA-induced protein regulation has shown therapeutic benefits in breast cancer.[17] The major stumbling block for the clinical siRNA therapy is its delivery to target cells. The short half-life ($t_{1/2}$ ~1.5 min[18]) of siRNA in blood and need for intracellular delivery are challenges for translation to the clinic. A variety of methods have been developed to deliver siRNA, including direct intravenous injection of "naked" or chemically stabilized siRNA,[19,20] packaging of siRNA into DNA plasmid vectors,[21,22] transposon vectors (transgenic plasmids),[23] plasmid-infected viruses,[24] virosomes (reconstituted viral envelopes),[25] lentiviral vectors,[26,27] and liposomes.[28] We have previously demonstrated that pH-responsive liposomes are advantageous for delivering siRNA, because they not only improve pharmacokinetics but also provide a stable shield from enzyme degradation.[29]

In this report, we hypothesized that a synergistic treatment coupled CXCR4 axis blockade and Lcn2 silencing could inhibit MBC cell migration more efficiently than either one of these treatments alone. The role of CXCR4 in our drug delivery system is 2-fold: (1) targeting CXCR4 overexpression on breast cancer cells, which may enhance therapeutic binding, and (2) inhibiting MBC metastasis by blocking the CXCR4 chemokine axis.[30] Targeting and inhibition of CXCR4 together with pH-triggered delivery of Lcn2 siRNA may be achieved in one vehicle. This multitargeted approach, which obstructs two migratory pathways, may be a novel and powerful strategy for inhibiting MBC migration.

EXPERIMENTAL SECTION

Materials. 1,2-Dioleoyl-3-dimethylammonium-propane (DODAP), 1,2-dioleoyl-*sn*-glycero-3-phosphocholine (DOPC), and 1,2-dioleoyl-*sn*-glycero-3-phosphoethanolamine-*N*-dodecanoyl (N-dod-PE) were obtained from Avanti Polar Lipids (Alabaster, AL). Immunoglobulin G (IgG) isotype control, mouse anti-human CXCR4 monoclonal antibody (aCXCR4), and NorthernLight 557 (NL557)-conjugated donkey anti-mouse IgG were purchased from R&D Systems (Minneapolis, MN). Triton X-100, 1-ethyl-3-(3-dimethylaminopropyl)carbodiimide hydrochloride (EDC), *N*-hydroxysuccinimide (NHS), bovine serum albumin (BSA), rhodamine-B isothiocyanate-conjugated dextran (rhodamine-dextran, 10 kDa MW), anhydrous dimethyl sulfoxide (DMSO), and ethanol (EtOH) were purchased from Sigma-Aldrich (St. Louis, MO). Phycoerythrin (PE)-conjugated mouse anti-human CXCR4 antibody (PE-aCXCR4) and PE-conjugated mouse IgG isotype (PE-IgG) were purchased from BioLegend (San Diego, CA). Formaldehyde was obtained from EMD Chemicals (Gibbstown, NJ). Dulbecco's phosphate buffered saline (PBS), 0.25% trypsin/2.6 mM ethylenediaminetetraacetic acid (EDTA) solution, human CXCR4 Taqman gene expression assay (Hs.593413), Gibco Dulbecco's modified Eagle medium (DMEM), GibcoDMEM/F12(1:1), 4′,6-diamidino-2-phenylindole (DAPI), Quant-iT RNA Assay Kit, Lipofectamine RNAiMAX Transfection Reagent, and CellTracker Green CMFDA (5-chloromethylfluorescein diacetate) were purchased from Invitrogen (Carlsbad, CA). Leibovitz's L-15 Medium and Roswell Park Memorial Institute (RPMI)-1640 Medium were obtained from ATCC (Manassas, VA). Lab-Tek II Chamber Slide System was obtained from Thermo Fisher Scientific (Pittsburgh, PA). Nuclepore track-etched membrane (pore size: 100 nm) was obtained from Whatman (Florham Park, NJ). FLOAT-A-LYZER G2 dialysis tubing (MWCO 300 kDa) was purchased from Spectrum Laboratories (Rancho Dominguez, CA). Slide-A-Lyzer dialysis cassette (MWCO 20 kDa) was obtained from Pierce Biotechnology (Rockford, IL). Quantum Simply Cellular microbeads were purchased from Bangs Laboratory, Inc. (Fishers, IN). Dojindo cell counting kit was purchased from Dojindo Molecular Technologies (Rockville, MD). Diff-Quik Stain Set was purchased from Siemens Healthcare Diagnostics (Tarrytown, NY). Fluorogel with tris buffer was purchased from Electron Microscopy Sciences Inc. (Hatfield, PA).

Cell Culture. HCC1500, MDA-MB-175VII, MDA-MB-436, MDA-MB-231, and MCF10A were obtained from American Type Culture Collection (ATCC, Manassas, VA) and cultured in RPMI-1640 medium, Leibovitz's L-15 medium, DMEM, and DMEM/F12(1:1) medium with supplements, respectively. All cells were cultured in a 37 °C humidified incubator with 5% CO_2.

The Sequence of Lcn2 siRNA. siGENOME SMARTpool human Lcn2 siRNA constructs and siGENOME Non-Targeting siRNA Pool were purchased from Dharmacon (Lafayette, CO). Lcn2 siGENOME SMARTpool siRNA is composed of four Lcn2 siRNAs: D-003679-05, UGGGCAACAUUAAGAGUUA; D-003679-03, GAAGACAAGAGCUACAAUG; D-003679-02, GGAGCUGACUUCGGAACUA; D-003679-01, GAGCUGACUUCGGAACUAA.

Quantification of CXCR4 and Lcn2 Gene Expression. RNA was collected with the Qiagen RNeasy minikit and quantified by a SpectraMaxPlus 384 UV−visible spectrophotometer (Molecular Devices Corp, Sunnyvale, CA). The PCR was performed by using a StepOnePlus Real-Time PCR System (Applied Biosystems, Carlsbad, CA). All PCR samples were referenced to the gene expression of glyceraldehyde 3-phosphate dehydrogenase (GAPDH).

Quantification of CXCR4 Surface Expression. Breast cancer cell CXCR4 surface expression was quantified by using Quantum Simply Cellular microbeads with the manufacturer's protocol. 10^6 cells were harvested and rinsed twice, and 1% bovine serum albumin (BSA) in PBS solution was used to block the cells for 30 min in an ice bath. Then cells were stained with PE-aCXCR4 antibody for 1 h at RT. After antibody staining, cells were rinsed with 1% BSA in PBS three times, resuspended in PBS, and evaluated by a BD FACSCalibur Flow Cytometer (BD Biosciences, San Jose, CA).

CXCR4 Immunofluorescent Staining. 2×10^5 cells were seeded in a Lab-Tek II Chamber Slide System overnight. Then cells were fixed with 4% formaldehyde in PBS at RT for 10 min and blocked with 1% BSA in PBS for 30 min in an ice bath. Resulting fixed cells were stained with mouse anti-human CXCR4 primary antibody and NorthernLight 557 conjugated goat anti-mouse secondary antibody, sequentially. DAPI was used to stain the cell nucleus. Fluorogel with tris buffer was used to mount the samples. Samples were examined under a Leica TCS SP5 confocal fluorescent microscope (Leica Microsystems, Buffalo Grove, IL).

CXCR4-Targeted, siRNA Encapsulating Liposome Preparation. DOPC, DODAP, and N-dod-PE were mixed at a mole ratio of 65:30:5 and dried in a rotary evaporator. Resulting 5 μmol thin film was redissolved in 1 mL of

DMSO:EtOH (7:3, v:v) and added to 9 mL of a solution of 15 μg/mL siGENOME SMARTpool human Lcn2 siRNA or siGENOME Non-Targeting siRNA (scrambled siRNA) in PBS (pH 7.4). After 10 freeze−thaw cycles, lipid solution was extruded via a NorthernLipids Extruder with a 100 nm polycarbonate nanoporous membrane. Obtained liposome solution was dialyzed in PBS using a Slide-A-Lyzer dialysis cassette (MWCO 20 kDa) overnight at RT.

2 mg of EDC and 3 mg of NHS were incubated with 1 mmol of lipid (liposomes) in PBS for 6 h at RT. A Slide-A-Lyzer dialysis cassette (MWCO 20 kDa) was used to remove unreacted EDC and NHS from the liposome solution. Then, aCXCR4 or the IgG control was added to EDC-modified liposomes at a molar ratio of 1:1000 (antibody:phospholipid) and incubated overnight at RT. Unreacted antibodies were removed by 24 h dialysis using a FLOAT-A-LYZER G2 dialysis tubing (MWCO 300 kDa). aCXCR4-labeled, rhodamine-dextran encapsulating liposomes (aCXCR4-RD-pHs) were also produced for liposome binding studies. Its preparation process is similar to that of aCXCR4-Lcn2-pHs except that 1 mL of lipid solution was added to a 9 mL rhodamine-dextran solution (1 mg/mL). Lcn2 siRNA encapsulated Lipofectamine (Lcn2-LIPO) was prepared using the manufacturer's protocol and used as a positive control.

aCXCR4 density on liposomes was quantified by borosilicate bead assay. 2 μm borosilicate beads were coated with a layer of lipids from liposomes by sonicating small unilamellar liposomes with microbeads in PBS for 6 h. PE-aCXCR4 or PE-IgG (nonspecific binding) was conjugated to liposome coated microbeads using the same EDC/NHS chemistry. aCXCR4 surface density on each microbead was evaluated by flow cytometry following a similar protocol for CXCR4 cell surface expression quantification. Dynamic light scattering was used to measure the liposome size and zeta potential with a Zeta-PALS analyzer (Brookhaven Instruments, Holtsville, NY) in PBS (pH 7.4).

siRNA Encapsulation Efficiency. A Quant-iT RiboGreen RNA assay (Invitrogen, Carlsbad, CA) was performed to determine the encapsulation efficiency of siRNA within the liposome samples by using the manufacturer's protocol. A siRNA concentration calibration curve was generated from a series of serially diluted siRNA standard solutions and appropriate backgrounds measured on a SpectraMaxPlus 384 UV−visible spectrophotometer (excitation 500 nm, emission 525 nm). Then a 20 μL liposome sample was added to 1 mL of 0.5% Triton X-100 in a microcentrifuge tube and vortexed for 1 min. The microcentrifuge tube was transferred to a 37 °C incubator for 1 h. Triton X-100 is a surfactant that lyses liposomes. Then, 200 μL of the siRNA containing Triton X-100 solution was homogeneously mixed with 200 μL of 200-fold diluted Quant-iT RiboGreen RNA reagent working solution for 5 min. Resulting mixture solution was added to at least three wells for each sample of a flat bottom 96-well cell culture plate and measured for fluorescence. The 0.5% Triton X-100 solution mixed with 200-fold diluted Quant-iT RiboGreen RNA reagent working solution was used as a blank control. The encapsulation efficiency is calculated from the following formula: encapsulated siRNA concentration/initial siRNA concentration ×100.

siRNA Sustained Release in Different pH. Release of siRNA from aCXCR4-Lcn2-pH and aCXCR4-Lcn2-LP were measured in PBS at pH 5.5 and 7.4 at 37 °C. pH value of PBS was adjusted by 1 M HCl. The aCXCR4-Lcn2-pH or aCXCR4-Lcn2-LP solution (1 mL, siRNA: 0.36 μM) was added to a FLOAT-A-LYZER G2 dialysis tubing (MWCO 300 kDa) and dialyzed in 30 mL of PBS (pH 5.5 or 7.4) at 37 °C on a shaker (100 rpm). 100 μL samples were collected from the solution outside the dialysis tube at different time points, and the siRNA concentration was quantified with Quant-iT RNA Assay Kit on a SpectraMaxGEMIN XPS fluorescence spectrophotometer (Molecular Devices Corp, Sunnyvale, CA).

Liposome Binding. HCC1500, MDA-MB-175VII, MDA-MB-436, MDA-MB-231, and MCF10A cells were seeded on 6-well plates at a density of 3×10^5 cells/well overnight. Then cells were incubated for 4 h at 37 °C with (1) rhodamine-dextran encapsulated nonspecific (IgG) liposome (IgG-RD-pH) and (2) aCXCR4-RD-pH at a concentration of 1 μmol lipid/10^6 cells. Then liposome binding efficiency was evaluated by flow cytometer and analyzed with FlowJo software. The fold-over IgG-RD-pH value was calculated by dividing the mean fluorescence intensity of aCXCR4-RD-pH stained cells by that of the IgG-RD-pH stained cells.

Cell-Liposome Immunofluorescent Staining. Immunofluorescent staining was performed as described previously in CXCR4 immunofluorescent staining section. Instead of using aCXCR4 antibody, cells were incubated for 4 h at 37 °C with (1) IgG-RD-pHs and (2) aCXCR4-RD-pHs, respectively.

Lcn2 siRNA Knockdown. 10^6 cells (HCC1500, MDA-MB-175VII, and MCF10A) or 10^5 cells (MDA-MB-436 and MDA-MB-231) were seeded in 6-well plates and incubated for 24 h. Cells were treated with (1) PBS; (2) naked siRNA; (3) aCXCR4-pH without siRNA; (4) aCXCR4-SCR-pH; (5) Lcn2-LIPO; (6) IgG-Lcn2-pH; (7) aCXCR4-Lcn2-LP; and (8) aCXCR4-Lcn2-pH for 6 h at the siRNA concentration of 72 pmol/10^6 cells (equivalent lipid concentration: 1 μmol/10^6 cells for aCXCR-pH, aCXCR-SCR-pH, IgG-Lcn2-pH, and aCXCR4-Lcn2-pH; 2.25 μmol/10^6 cells for aCXCR-Lcn2-LP; 0.5 μmol/10^6 cells for Lcn2-LIPO). Cells were rinsed three times with PBS and further grown for 72 h. Lcn2 gene expression was determined by qRT-PCR.

In the liposome concentration dependence tests, MDA-MB-436 and MDA-MB-231 cells were treated with aCXCR4-Lcn2-pH for 6 h at three different lipid concentrations: 0.25, 0.5, and 1 μmol/10^6 cells. The siRNA concentration was different between samples: aCXCR4-Lcn2-pH, aCXCR4-SCR-pH, and Lcn2-LIPO had 72, 70, and 140 pmol per μmol of lipid, respectively. Cells were rinsed three times with PBS and further grown for 72 h. The Lcn2 gene expression was examined by qRT-PCR.

Cell Migration. Two aggressive MBC cells, MDA-MB-436 and MDA-MB-231, were treated with (1) PBS; (2) naked siRNA; (3) aCXCR4-pH without siRNA; (4) aCXCR4-SCR-pH; (5) Lcn2-LIPO; (6) IgG-Lcn2-pH; (7) aCXCR4-Lcn2-LP; and (8) aCXCR4-Lcn2-pH for 6 h at the siRNA concentration of 72 pmol/10^6 cells. Cells were rinsed three times with PBS and further grown for 72 h. MDA-MB-436 (10^5 cell per well) or MDA-MB-231 (50,000 cell per well) cells were seeded onto COSTAR Transwell insert with permeable support polycarbonate membrane with 8 μm pore size in a 24-well plate. DMEM without or with 10% fetal bovine serum was added to the upper and lower wells respectively. Cells were incubated and allowed to migrate for 20 h. Then cells on the reverse side of the Transwell membrane facing the lower chamber after transmigrating through the 8 μm pores of the Transwell membrane were stained with Diff-Quik Stain Set. Three fields were counted for each sample.

In liposome concentration dependence tests, MDA-MB-436 and MDA-MB-231 cells were treated with aCXCR4-Lcn2-pH for 6 h at three different lipid concentrations: 0.25, 0.5, and 1 μmol/10^6 cells. Cells were rinsed three times with PBS and further grown for 72 h. Cell migration was examined by Transwell migration assay as described above.

Cytotoxicity. In liposome concentration dependence tests, MDA-MB-436 and MDA-MB-231 cells were treated with aCXCR4-Lcn2-pH for 6 h at three different lipid concentrations: 0.25, 0.5, and 1 μmol/10^6 cells. Cells were rinsed three times with PBS and further grown for 72 h. The cytotoxicity of liposome treated cells was evaluated by Dojindo cytotoxicity assay with the manufacturer's protocol.

Statistical Analysis. Data were measured in at least triplicate and presented as mean ± standard deviation. Statistical analysis was performed by using Student's *t*-test. *P* values <0.05 were considered statistically significant.

RESULTS AND DISCUSSION

CXCR4 was previously identified as being significantly overexpressed in human breast tumor samples by immunohistochemical staining (IHC).[31] In our study, we characterized the CXCR4 gene and surface expression in four MBC cell lines: HCC1500, MDA-MB-175VII, MDA-MB-436, and MDA-MB-231. HCC1500 is estrogen receptor (ER)+/progesterone receptor (PR)+/HER2−; MDA-MB-175VII is ER+/PR−/HER2−; and MDA-MB-436 and MDA-MB-231 are triple-negative (ER−/PR−/HER2−). The non-neoplastic mammary epithelial cell line, MCF10A, was used as a control. CXCR4 gene expression was quantified relative to MCF10A by qRT-PCR. As shown in Figure 1A, HCC1500, MDA-MB-175VII, MDA-MB-436, and MDA-MB-231 exhibited 10-, 2.5-, 3.7-, and 2.8-fold higher CXCR4 gene expression than MCF10A, respectively.

The CXCR4 surface density was quantified via flow cytometry using a microbead assay (Table 1).[32] Similar to their CXCR4 gene expression levels, MBC cell lines demonstrated significantly higher CXCR4 surface expression than MCF10A. CXCR4 surface expression in HCC1500 and MDA-MB-175VII was over 20-fold higher than MCF10A. The most aggressive, triple-negative MDA-MB-231 cells had considerably less CXCR4 surface expression than both HCC1500 and MDA-MB-175VII cells. This suggested that MBC aggressiveness may be independent of the CXCR4 surface density.

CXCR4 surface expression in MBC cells was further confirmed via immunofluorescent staining. Representative micrographs illustrated greater CXCR4 surface expression on HCC1500, MDA-MB-175VII, MDA-MB-436, and MDA-MB-231 (Figure 1B−M) relative to MCF10A (Figure 1N−P). These data confirm that CXCR4 is overexpressed on the cell surface of MBC cells but not non-neoplastic MCF10A cells. CXCR4 expression in leukocytes, endothelial cells, and hematopoietic stem cells is lower than cancer cells.[33−37] Therefore, CXCR4 may be a novel and desirable target for MBC cells. We have shown previously that CXCR4 surface expression—not gene expression—was a better predictor of *in vitro* liposome binding.[38]

We engineered CXCR4-targeting, Lcn2 siRNA-encapsulating, pH-responsive liposomes to test our synergistic therapeutic hypothesis. A schematic diagram is shown in Figure 2. pH-responsive liposomes are composed of a mixture of 1,2-dioleoyl-*sn*-glycero-3-phosphocholine (DOPC), 1,2-dioleoyl-3-dimethylammonium-propane (DODAP, pK_a 6.6[39]), and 1,2-dioleoyl-*sn*-glycero-3-phosphoethanolamine-*N*-dodecanoyl (N-dod-PE) (65:30:5, mol:mol:mol). Liposomes incorporating DODAP respond to the

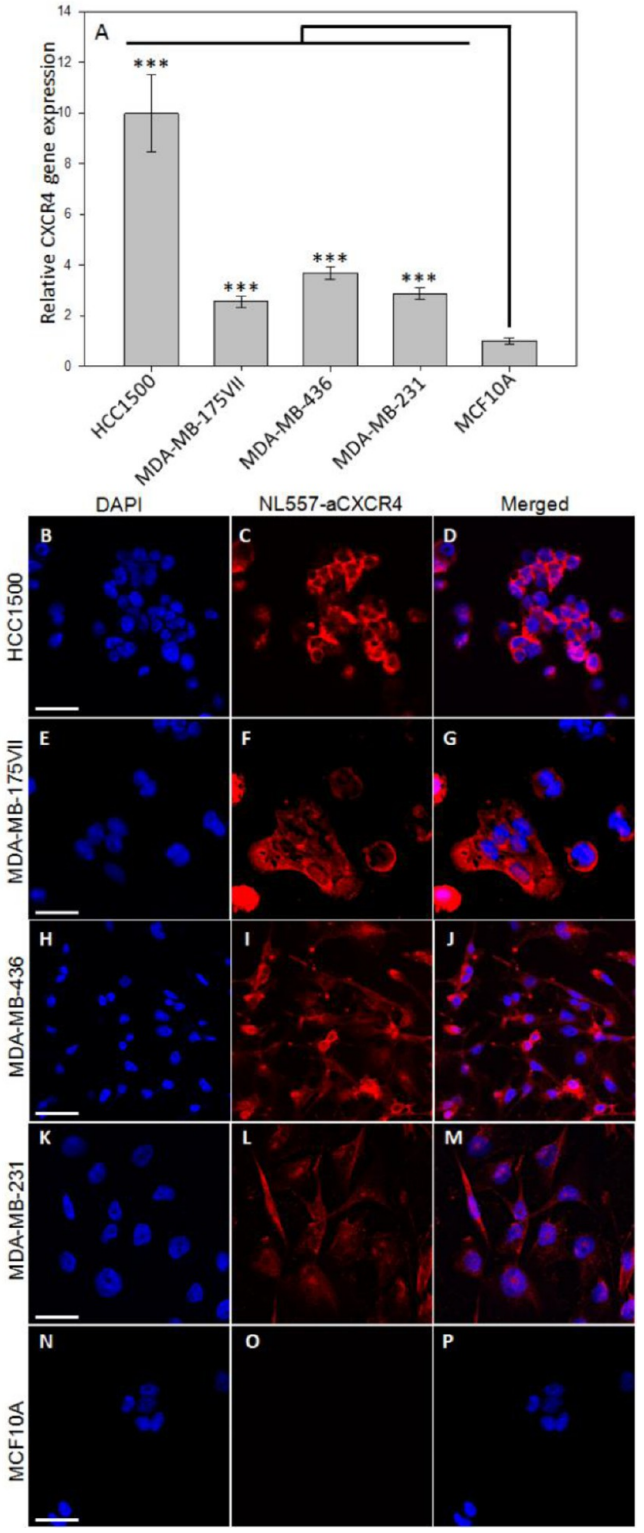

Figure 1. Characterization of CXCR4 gene and surface expression on metastatic breast cancer and normal breast epithelial cells. CXCR4 gene expression was quantified by qRT-PCR in panel A. CXCR4 fold change is relative to GAPDH (*** $p < 0.001$). Panels B−P are representative confocal fluorescence microscope images of CXCR4 immunofluorescent staining in HCC1500 (B−D); MDA-MB-175VII (E−G); MDA-MB-436 (H−J); MDA-MB-231 (K−M); and MCF10A (N−P). DAPI was used to stained the cell nuclei; mouse anti-human CXCR4 antibody (primary) and goat anti-mouse NL557 antibody (secondary) were used to stain CXCR4. All scale bars in panels B−P represent 20 μm.

dx.doi.org/10.1021/mp4004699 | *Mol. Pharmaceutics* 2014, 11, 755−765

Table 1. CXCR4 Surface Density on MBC Cells

	HCC1500	MDA-MB-175VII	MDA-MB-436	MDA-MB-231	MCF10A
CXCR4 (molecules/cell)	104,600 ± 680	110,000 ± 1,000	59,000 ± 1,400	15,000 ± 1,000	4,600 ± 100

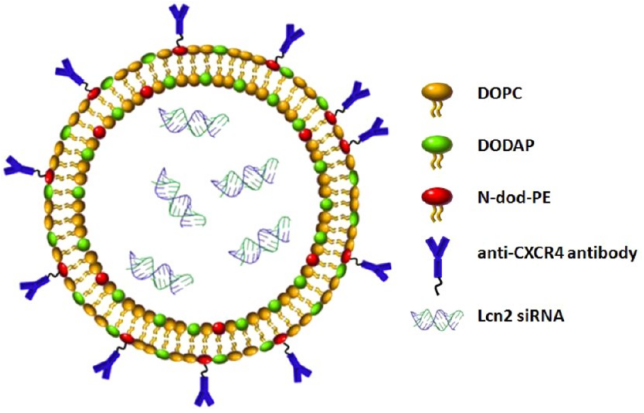

Figure 2. Schematic diagram of aCXCR4-Lcn2-pH.

acidic endosomal environment[40,41] by increasing their cationic character, fusing with the endosomal membrane, and delivering the encapsulated siRNA within the cytoplasm.[29] N-dod-PE was selected as the anchor for either an anti-CXCR4 antibody (aCXCR4) or a nonspecific immunoglobulin G (IgG) conjugation. EDC/NHS chemistry was used to covalently bond the carboxylic acid on N-dod-PE to a primary amine group present on aCXCR4 or IgG, which is a widely used approach to modify liposomes.[42] Conjugated aCXCR4 antibodies can target liposomes specifically to CXCR4 overexpressing MBC cells and simultaneously inhibit the CXCR4 chemokine axis. siGENOME SMARTpool human Lcn2 siRNA was encapsulated within the liposome by directly mixing siRNA solubilized in PBS with the dry lipid film during liposome preparation. A nonresponsive liposome comprised of DOPC:N-dod-PE (95:5, mol:mol) was used as a control.

Liposome formulations were prepared and tested to compare the efficacy of siRNA delivery: (1) aCXCR4-targeted, Lcn2 siRNA encapsulating, pH-responsive liposome (aCXCR4-Lcn2-pH); (2) aCXCR4-targeted, Lcn2 siRNA encapsulating, nonresponsive liposome (aCXCR4-Lcn2-LP); (3) CXCR4-targeted, scrambled siRNA encapsulating, pH sensitive liposomes (aCXCR4-SCR-pH); and (4) Lcn2 siRNA encapsulating, Lipofectamine complexes (Lcn2-LIPO). aCXCR4-Lcn2-LP and aCXCR4-SCR-pH were used as negative controls, and Lcn2-LIPO was a positive control. Their physical characteristics are shown in Table 2. The hydrodynamic diameters of aCXCR4-Lcn2-pH, aCXCR4-Lcn2-LP, aCXCR4-SCR-pH, and Lcn2-LIPO were 132 ± 4, 103 ± 2, 134 ± 3, and 703 ± 345 nm, respectively, as determined by dynamic light scattering (DLS). Liposomes with diameters of less than 200 nm are ideal for intravenous administration due to their enhanced permeability and retention (EPR) within tumors.[39] The polydispersity index (PDI) of all three extruded liposomes was less than 0.1, demonstrating uniformity. Lipofectamine complexes are routinely larger and less uniform due to the aggregation of cationic molecules with negatively charged siRNA.[43] The zeta potentials of aCXCR4-Lcn2-pH and aCXCR4-Lcn2-LP were −5.4 ± 1.4 and −2.4 ± 0.4 mV, respectively, which were close to neutral charge. The siRNA encapsulation efficiencies of aCXCR4-Lcn2-pH (36 ± 4%) and aCXCR4-SCR-pH (35 ± 6%) were significantly higher than that of aCXCR4-Lcn2-LP (16 ± 7%). Lcn2-LIPO had a higher encapsulation efficiency of 70 ± 2%. The antibody surface density was 2,200 ± 190 molecules/μm^2 for aCXCR4-Lcn2-pH and aCXCR4-SCR-pH compared to 1,720 ± 20 molecules/μm^2 for aCXCR4-Lcn2-LP. aCXCR4-SCR-pH had similar parameters to aCXCR4-Lcn2-pH due to the same liposome composition, albeit with the exception of loaded siRNA.

Release profiles of Lcn2 siRNA from aCXCR4-Lcn2-pH and aCXCR4-Lcn2-LP were determined by measuring the siRNA

Table 2. Diameter, Size Distribution, Zeta Potential, siRNA Loading, and Antibody Density of Prepared Liposomes

sample	size (nm)	polydispersity index	zeta potential (mV)	encapsulation efficiency (%)	aCXCR4 antibody density (molecules/μm^2)
aCXCR4-Lcn2-pH	132 ± 4	0.05	−5.4 ± 1.4	36 ± 4	2,200 ± 190
aCXCR4-Lcn2-LP	103 ± 2	0.06	−2.4 ± 0.4	16 ± 7	1,720 ± 20
aCXCR4-SCR-pH	134 ± 3	0.04	−4.3 ± 0.2	35 ± 6	2,200 ± 190
Lcn2-LIPO	703 ± 345	0.273	−3.4 ± 2.5	70 ± 2	N/A

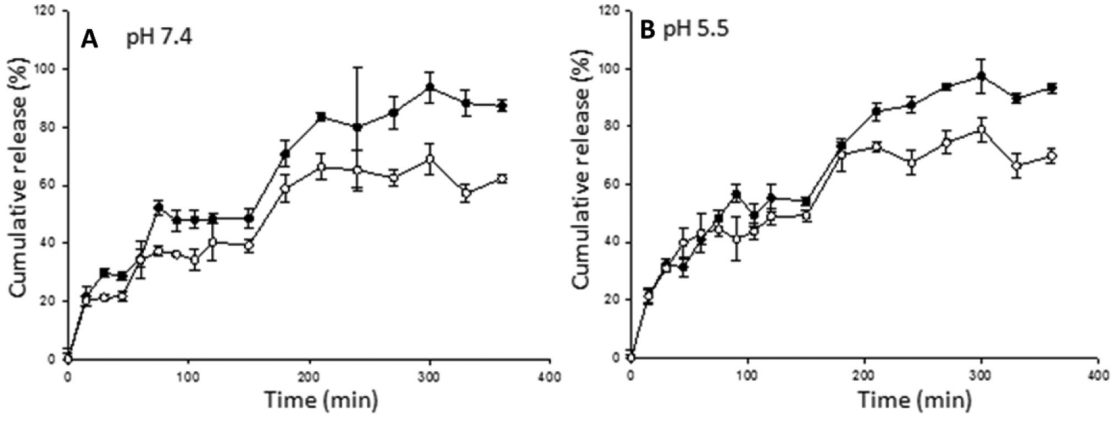

Figure 3. Cumulative siRNA releases from aCXCR4-Lcn2-pH (●) and aCXCR4-Lcn2-LP (○) in pH 7.4 (A) and pH 5.5 (B) buffers at 37 °C.

dx.doi.org/10.1021/mp4004699 | Mol. Pharmaceutics 2014, 11, 755−765

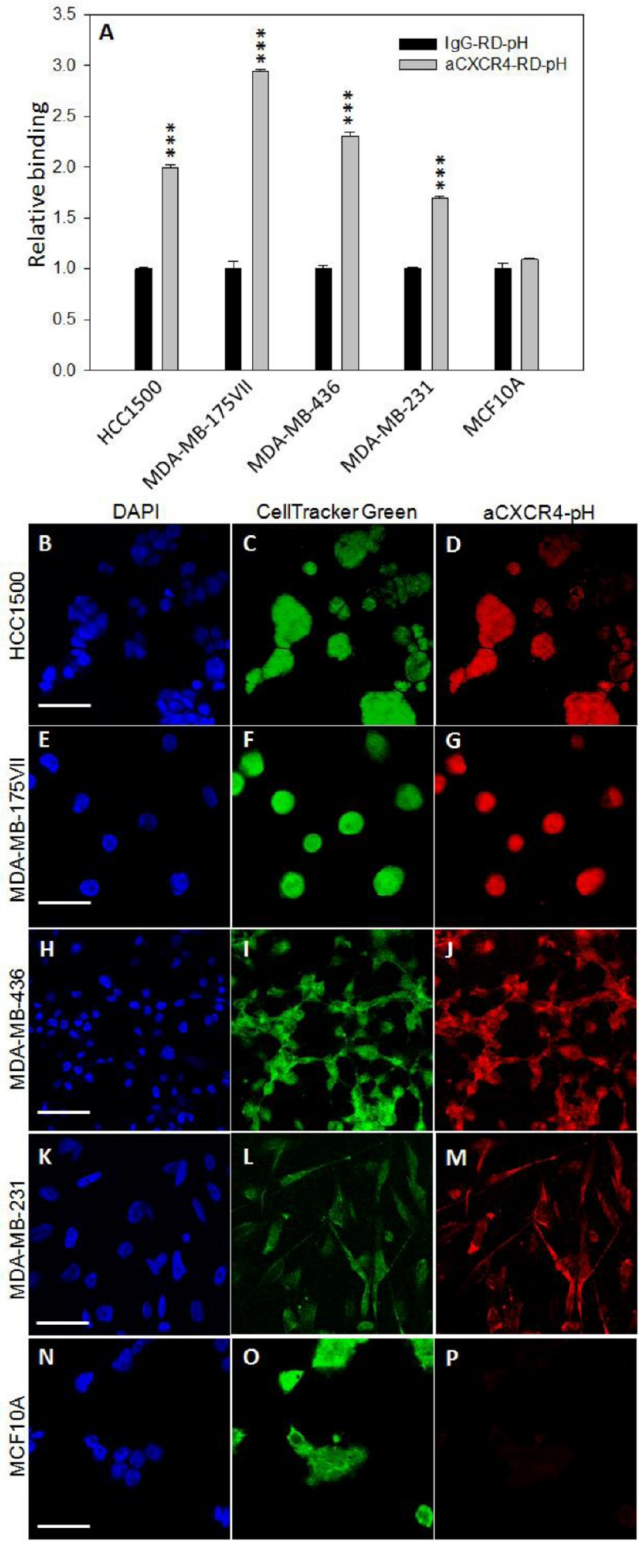

Figure 4. (A) Cellular binding of immunoliposomes in HCC1500, MDA-MB-175VII, MDA-MB-436, MDA-MB-231, and MCF10A. Cells were treated with aCXCR4-RD-pH and IgG-RD- pH (control) and then characterized via flow cytometry (*** $p < 0.001$). Panels B–P are representative confocal fluorescent microscope images of immunoliposome cellular binding in HCC1500 (B–D), MDA-MB-175VII (E–G), MDA-MB-436 (H–J), MDA-MB-231 (K–M), and MCF10A (N–P). DAPI and CellTracker Green were used to stain cell nuclei and cytoplasm, respectively. All scale bars in panels B–P represent 20 μm.

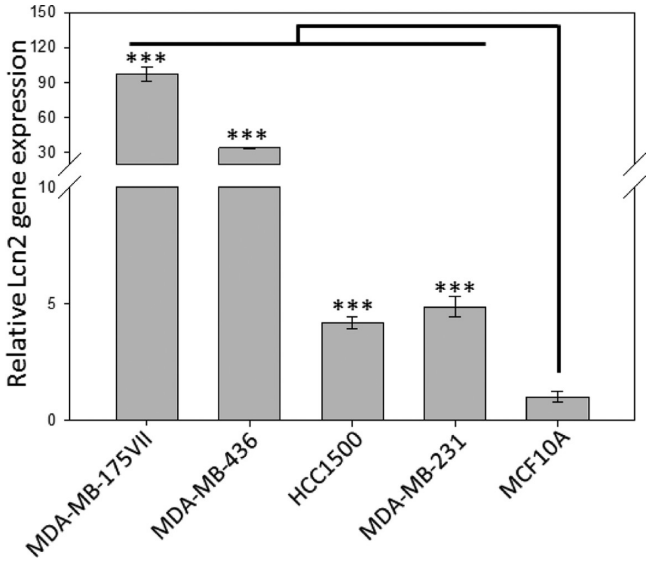

Figure 5. Lcn2 gene expression in MDA-MB-175VII, MDA-MB-436, HCC1500, MDA-MB-231, and MCF10A cells as quantified by RT-qPCR. Lcn2 fold change is relative to GAPDH (*** $p < 0.001$).

concentration after dialysis (Figures 3 and S1 in the Supporting Information). At pH 7.4, 50% of Lcn2 siRNA was released in 75 min from aCXCR4-Lcn2-pH, whereas it took 170 min for 50% of Lcn2 siRNA to be released from aCXCR4-Lcn2-LP. Similar results were obtained at pH 5.5. In the absence of a membrane with which to fuse,[26] siRNA release from aCXCR4-Lcn2-pH and aCXCR4-Lcn2-LP was independent of pH. We have previously demonstrated that this pH-responsive formulation could successfully deliver siRNA to HeLa and HUVEC cells in comparison with nonresponsive liposomes.[26] In addition, the zeta-potential of aCXCR4-Lcn2-pH changed from -5.4 ± 1.4 mV (pH 7.4) to 13.9 ± 0.6 mV (pH 5.5); whereas that of aCXCR4-Lcn2-LP merely changed from -2.4 ± 0.4 mV (pH 7.4) to 0.6 ± 1.9 mV (pH 5.5). The increased cationic character of the aCXCR4-Lcn2-pH liposomes may result in electrostatic interactions between the siRNA and lipids, limiting their ability to dialyze through the membrane.

Quantification of liposome binding to MBC cells was performed to evaluate the targeting effectiveness of aCXCR4-conjugated liposomes. In this study, aCXCR4 antibody or IgG labeled, rhodamine dextran (RD) encapsulating, pH-responsive liposomes (aCXCR4-RD-pH or IgG-RD-pH) were prepared and used to quantitatively assess the MBC cellular binding and uptake of liposomes by flow cytometry. As shown in Figure 4A, HCC1500, MDA-MB-175VII, MDA-MB-436, and MDA-MB-231 cells demonstrated 2-, 2.9-, 2.3-, and 1.7-fold higher binding of CXCR4-targeted liposomes diluted in medium containing 10% serum relative to nonspecific IgG labeled liposomes, respectively. No difference was observed in MCF10A cells. Representative micrographs illustrate high aCXCR4-RD-pH binding on HCC1500, MDA-MB-175VII, MDA-MB-436, and MDA-MB-231 (Figure 4B–M) and low aCXCR4-RD-pH binding on MCF10A (Figures 4N–P). The shape and morphology of cell nuclei and whole cells are shown in blue and green fluorescence, respectively. The images indicate rounded and elongated cell morphologies. Rhodamine-dextran from aCXCR4-RD-pH is indicated by red fluorescence. In MBC cells (Figure 4B–M), red and green signals are overlapping. This suggests the release of the rhodamine-dextran

dx.doi.org/10.1021/mp4004699 | Mol. Pharmaceutics 2014, 11, 755–765

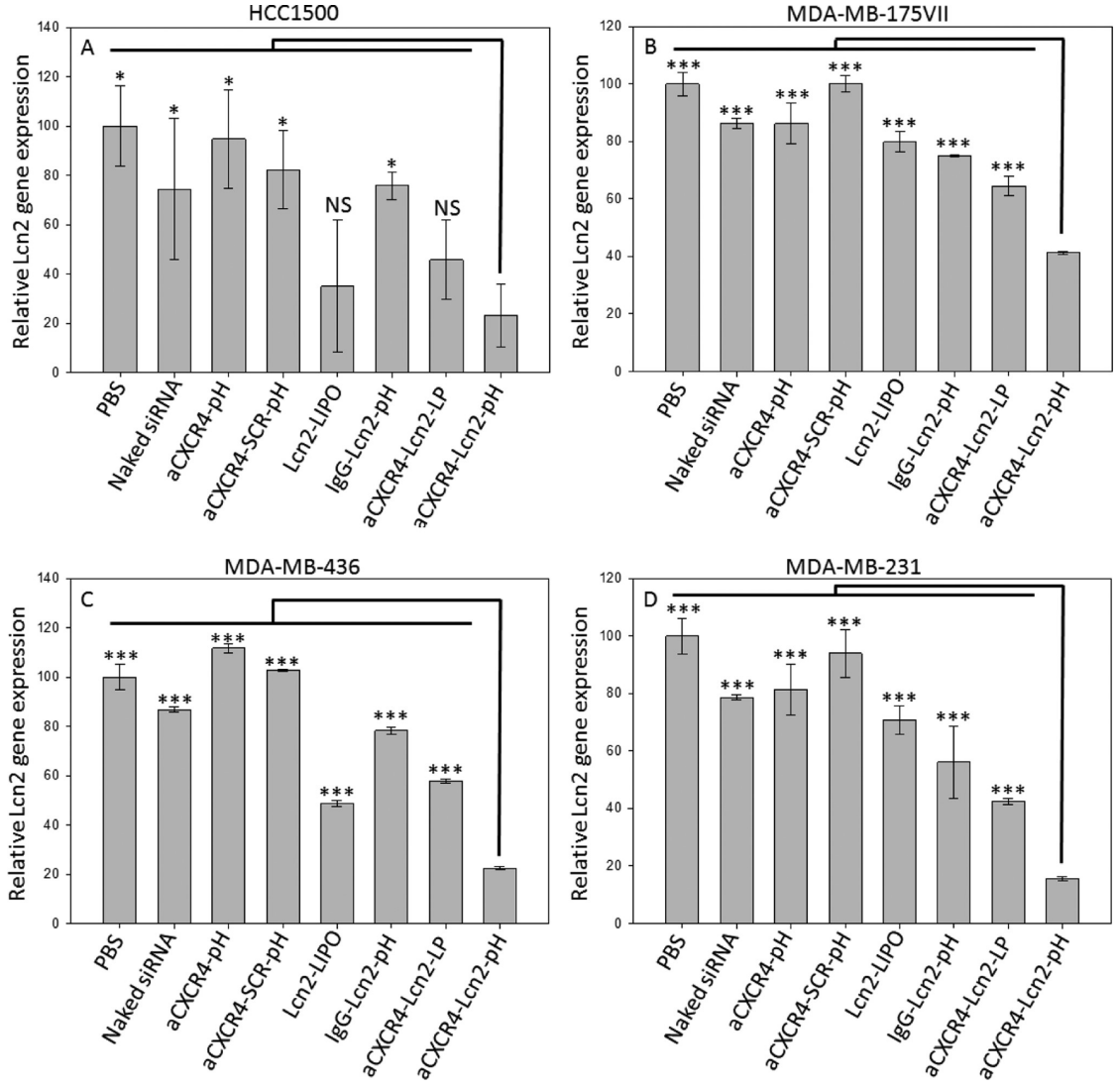

Figure 6. siRNA knockdown of Lcn2 gene expression in (A) HCC1500, (B) MDA-MB-175VII, (C) MDA-MB-436, and (D) MDA-MB-231 (NS: no significant difference, * $p < 0.05$, *** $p < 0.001$).

from aCXCR4-RD-pH and escape from endosomes into the cytoplasm. These results demonstrated that aCXCR4-RD-pH liposomes targeted MBC cells, not non-neoplastic cells. This was consistent with the high CXCR4 surface densities measured on MBC cells relative to MCF10A (Table 1).

In addition to targeting CXCR4, pH-triggered siRNA delivery was employed to silence the Lcn2 gene in MBC cells. The silencing effect was quantified by qRT-PCR. Figure 5 depicts endogenous Lcn2 expression in MBC cells before siRNA knockdown. MDA-MB-175VII, MDA-MB-436, HCC1500, and MDA-MB-231 exhibited 96-, 34-, 4.2-, and 4.9-fold higher Lcn2 gene expression than MCF10A, respectively. MBC cells were dosed for 6 h with aCXCR4-Lcn2-pH, rinsed, and then incubated for 72 h. MBC cells treated with aCXCR4-Lcn2-pH were compared to cells treated with PBS, naked Lcn2 siRNA, CXCR4-targeting, pH-responsive liposomes without Lcn2 siRNA (aCXCR4-pH), aCXCR4-SCR-pH, IgG-labeled, pH-responsive liposomes (IgG-Lcn2-pH), Lcn2-LIPO, and nonresponsive aCXCR4-Lcn2-LP at an equivalent siRNA concentration of 72 pmol per 10^6 cells. As shown in Figure 6A–D, MBC cells treated with aCXCR4-Lcn2-pH demonstrated the maximum Lcn2 gene knockdown: 78% for HCC1500, 65% for MDA-MB-175VII, 78% for MDA-MB-436, and 84% for MDA-MB-231. By comparison with the commercial siRNA transfection reagent, Lcn2-LIPO demonstrated lower gene knockdown (65% for HCC1500, 20% for MDA-MB-175VII, 51% for MDA-MB-436, and 30% for MDA-MB-231) after the 6 h dosing. MBC cells treated with nonresponsive aCXCR4-Lcn2-LP demonstrated knockdown in the range of 35–58%; this suggested that the pH-sensitive liposome is advantageous in siRNA delivery. MBC cells treated with nonspecific IgG-Lcn2-pH alone showed a 22–45% Lcn2 knockdown, significantly lower than those of CXCR4-targeted, pH-triggered, siRNA encapsulating liposomes. Similar to naked siRNA, aCXCR4-pH (without siRNA) and aCXCR4-SCR-pH (with nontargeting siRNA) demonstrated no significant reduction in Lcn2 expression, which confirmed that the CXCR4-CXCL12 axis blockade is independent of Lcn2 gene expression. The significant and efficient decrease in Lcn2 expression by aCXCR4-Lcn2-pH was achieved by employing both CXCR4 targeting and a pH-responsive nanocarrier.

We evaluated the synergistic effect of targeted Lcn2 siRNA delivery and CXCR4 chemokine axis blockade on MBC cell migration *in vitro*. Two aggressive triple-negative MBC cell lines, MDA-MB-436 and MDA-MB-231, were selected to test

dx.doi.org/10.1021/mp4004699 | *Mol. Pharmaceutics* 2014, 11, 755–765

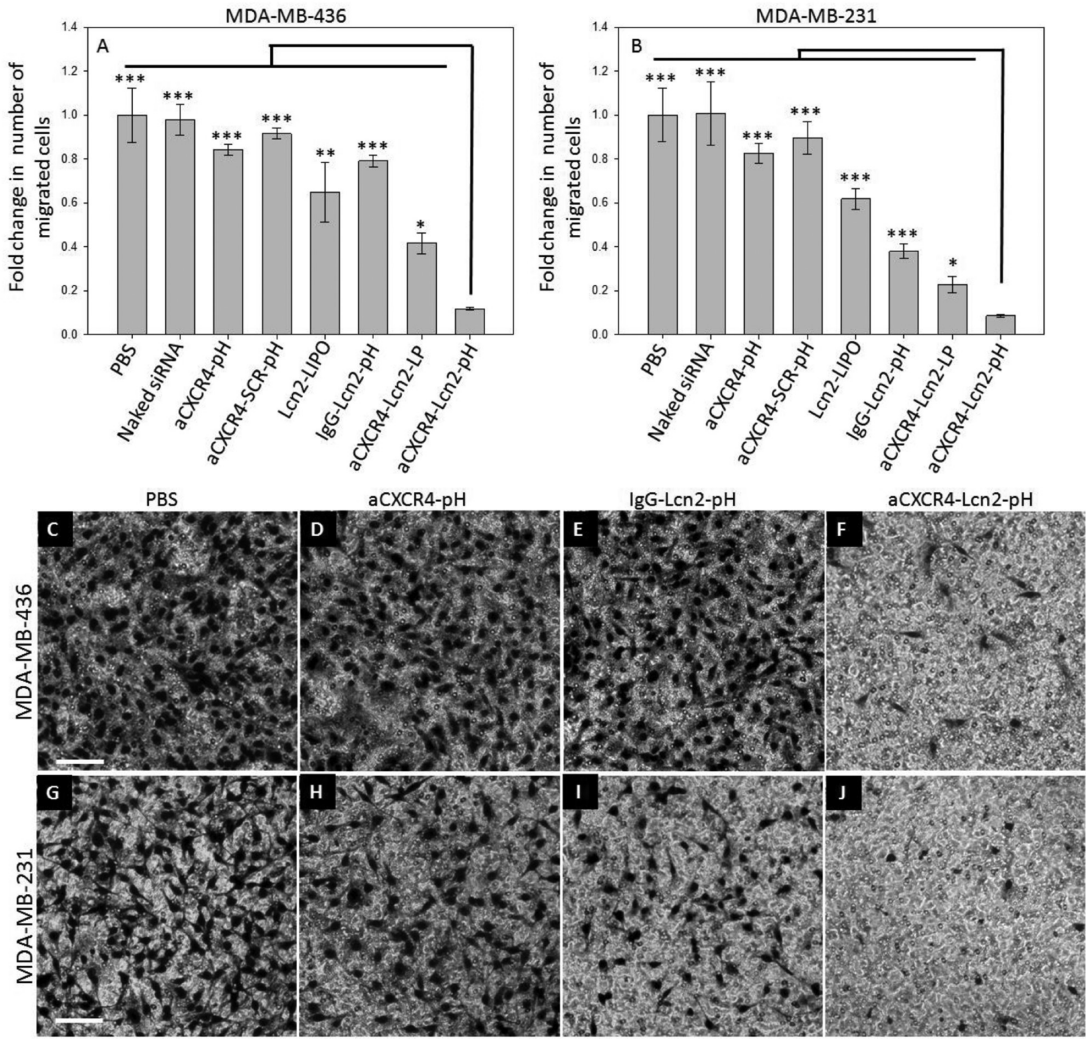

Figure 7. MDA-MB-436 (A) and MDA-MB-231 (B) cell migration were evaluated by Transwell migration assay. Both cells were incubated with PBS, naked siRNA, aCXCR4-pH, aCXCR4-SCR-pH, Lcn2-LIPO, IgG-Lcn2-pH, aCXCR4-Lcn2-LP, and aCXCR4-Lcn2-pH. Representative micrographs demonstrate MDA-MB-436 and MDA-MB-231 cells incubated with PBS (C and G), aCXCR4-pH (D and H), IgG-Lcn2-pH (E and I), and aCXCR4-Lcn2-pH (F and J), after transmigrating through 8 μm pores of a Transwell membrane. Images taken were on the reverse side of the membrane facing the lower chamber. All scale bars are 50 μm (* $p < 0.05$, ** $p < 0.01$, *** $p < 0.001$).

the therapeutic impact on migration in a Transwell migration assay. As shown in Figure 7, the number of migrated cells was significantly reduced in cells treated with aCXCR4-Lcn2-pH by 88% (MDA-MB-436) and 92% (MDA-MB-231) compared with untreated cells. This result is significantly higher than that achieved by the commercial transfection reagent Lipofectamine (Lcn2-LIPO, 35−38% inhibition). Cells treated with non-responsive aCXCR4-Lcn2-LP exhibited a 58% (MDA-MB-436) and a 77% (MDA-MB-231) decrease. No significant changes in cell migration were observed in cells treated with PBS and naked siRNA. These results are consistent with the siRNA knockdown study (Figure 6). Cells treated with aCXCR4-pH, aCXCR4-SCR-pH, and IgG-Lcn2-pH demonstrated 16−18%, 9−10%, and 21−62% reductions in cell migration, respectively. Targeting the Lcn2 siRNA via the CXCR4 receptor was more effective in reducing cell migration than the use of the pH-responsive liposome (aCXCR4-Lcn2-LP vs IgG-Lcn2-pH). These data indicate that the combination of targeting and inhibition of CXCR4 and silencing of Lcn2 via aCXCR4-Lcn2-pH more effectively and synergistically impeded breast cancer cell migration than subverting a single migration pathway, either by knockdown of Lcn2 or inhibition of CXCR4 alone. Since metastasis inversely correlates with patient survival, a therapeutic directed at blocking multiple migratory pathways may prolong life.

aCXCR4-Lcn2-pH was selected as the optimal formulation for inhibiting MBC cell migration. First, we investigated the cytotoxicity of aCXCR4-Lcn2-pH in MDA-MB-436 and MDA-MB-231 cells via the Dojindo assay at equivalent lipid concentrations: 1, 0.5, and 0.25 μmol per 10^6 cells. aCXCR4-SCR-pH and Lcn2-LIPO were also studied. As shown in Figure 8A,B, no cytotoxicity was observed at all three lipid concentrations. The siRNA concentration was different between samples: aCXCR4-Lcn2-pH, aCXCR4-SCR-pH, and Lcn2-LIPO had 72, 70, and 140 μmol/mol lipid, respectively. Second, we determined the impact of the aCXCR4-Lcn2-pH concentration on Lcn2 gene knockdown (Figure 8C,D). A dose-dependent response was observed: Lcn2 gene expression decreased as the concentration of aCXCR4-Lcn2-pH increased. aCXCR4-Lcn2-pH at 1 μmol/10^6 cells (highest lipid concentration) demonstrated the highest Lcn2 gene knockdown efficiencies (78% for MDA-MB-436 and 84% for MDA-MB-231). Third, we

dx.doi.org/10.1021/mp4004699 | *Mol. Pharmaceutics* 2014, 11, 755−765

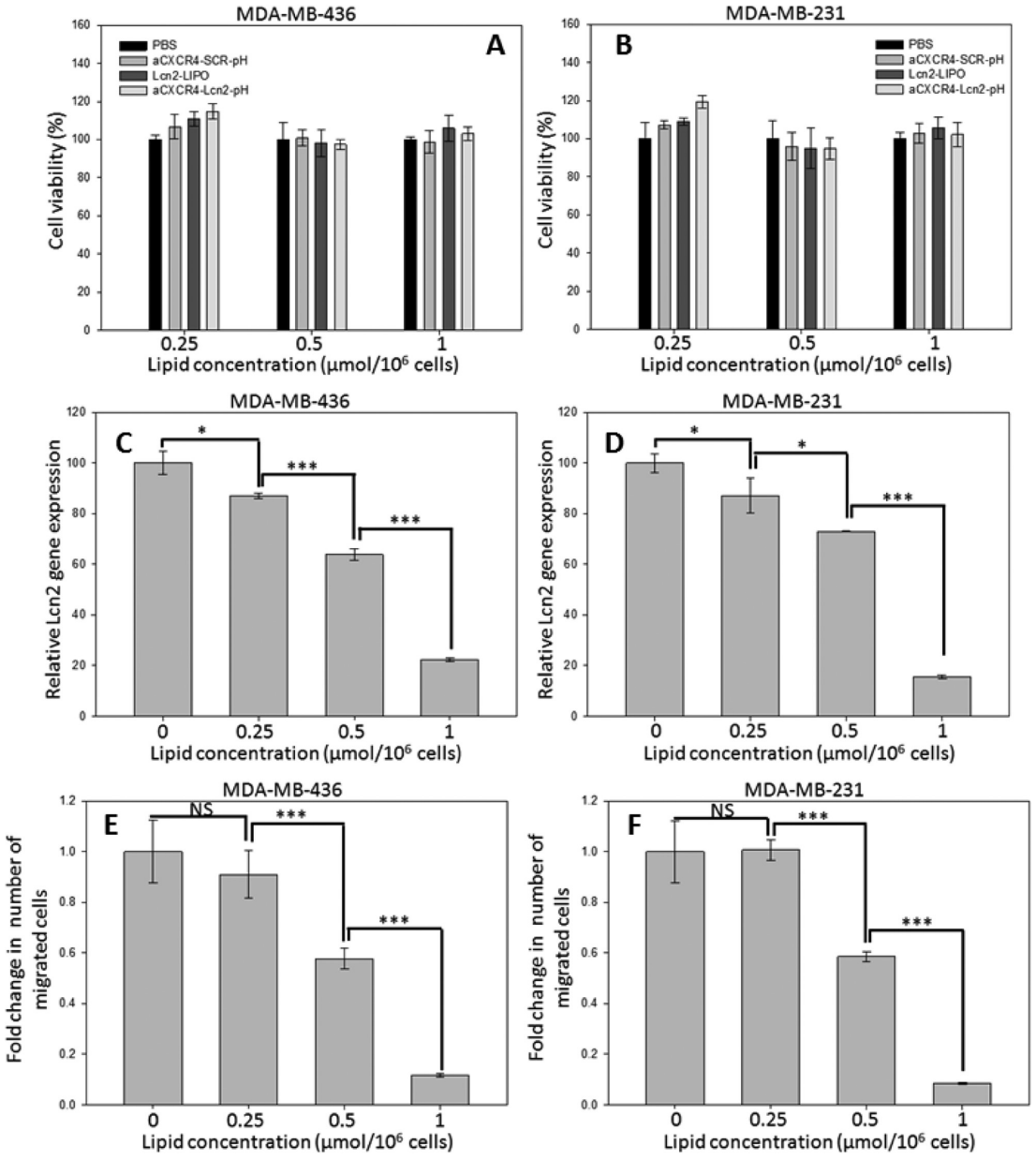

Figure 8. Lipid concentration dependence of MBC cell cytotoxicity (A and B), Lcn2 gene knockdown (C and D), and migration inhibition (E and F) (NS: no significant difference, $*p < 0.05$, $***p < 0.001$).

measured MBC cell migration inhibition as a function of aCXCR4-Lcn2-pH concentration. MBC cell migration inhibition (Figure 8E,F) correlated with Lcn2 gene knockdown. aCXCR4-Lcn2-pH at 1 μmol/10^6 cells demonstrated a 78−84% decrease in Lcn2 expression and an 88−92% decrease in MBC cell migration. The synergistic effects produced by blocking both CXCR4 and Lcn2 (Figure 7) may be due to the common signaling pathways that are activated by both molecules. Lcn2 promotes MBC cell migration by inducing the EMT.[15] The EMT has also been shown to be one of the mechanisms via which CXCL12/CXCR4 regulates breast cancer cell migration.[44] Evidence has suggested that CXCR4 may induce the EMT through the same transcription factor Slug as does Lcn2.[45,46] In addition, Lcn2 has also been reported to promote cancer cell migration by activating the Akt pathway,[47] which could also be activated by CXCR4.[48] The main limitation of the aCXCR4-Lcn2-pH approach would be unspecific binding to other CXCR4-expressing cells, e.g., leukocytes, endothelial cells, and hematopoietic stem cells. In the future, we will continue to investigate this synergistic inhibition strategy for MBC therapy in live animals.

■ CONCLUSIONS

We investigated the impact of simultaneous inhibition of CXCR4 and Lcn2 pathways on MBC cell migration via delivering CXCR4-targeted, pH-responsive liposomes encapsulating Lcn2 siRNA to multiple MBC cell lines. By using this method, the migration of two MBC cell lines, MDA-MB-436 and MDA-MB-231, was inhibited by 88% and 92%, respectively. This result is significantly more efficient than inhibition of the CXCR4 or Lcn2 pathway alone. Our results indicated that a synergistic therapy involving multiple migration pathways may be more successful than traditional therapies that focus on a singular approach.

dx.doi.org/10.1021/mp4004699 | *Mol. Pharmaceutics* 2014, 11, 755−765

■ ASSOCIATED CONTENT

Supporting Information

Figure S1 depicting free siRNA release profile in pH 7.4 and 5.5 buffers at 37 °C. This material is available free of charge via the Internet at http://pubs.acs.org.

■ AUTHOR INFORMATION

Corresponding Author

*Tel: +1-212-650-7169. Fax: +1-212-650-6727. E-mail: dauguste@ccny.cuny.edu.

Notes

The authors declare no competing financial interest.

■ ACKNOWLEDGMENTS

D.T.A. acknowledges the support of NIH (NCI 1DP2CA174495). M.A.M. acknowledges the support of the Breast Cancer Research Foundation.

■ REFERENCES

(1) Siegel, R.; Naishadham, D.; Jemal, A. Cancer Statistics, 2012. *Ca—Cancer J. Clin.* **2012**, *62*, 10−29.

(2) Perez, E. A.; Spano, J.-P. Current and Emerging Targeted Therapies for Metastatic Breast Cancer. *Cancer* **2012**, *118*, 3014−3025.

(3) Carter, C. L.; Allen, C.; Henson, D. E. Relation of Tumor Size, Lymph Node Status, and Survival in 24,740 Breast Cancer Cases. *Cancer* **1989**, *63*, 181−187.

(4) Vogel, C. L. Efficacy and Safety of Trastuzumab as a Single Agent in First-Line Treatment of HER2-Overexpressing Metastatic Breast Cancer. *J. Clin. Oncol.* **2002**, *20*, 719−726.

(5) Geyer, C. E.; Forster, J.; Lindquist, D.; Chan, S.; Romieu, C. G.; Pienkowski, T.; Jagiello-Gruszfeld, A.; Crown, J.; Chan, A.; Kaufman, B.; Skarlos, D.; Campone, M.; Davidson, N.; Berger, M.; Oliva, C.; Rubin, S. D.; Stein, S.; Cameron, D. Lapatinib plus Capecitabine for HER2-Positive Advanced Breast Cancer. *N. Engl. J. Med.* **2006**, *355*, 2733−2743.

(6) Awada, A.; Dirix, L.; Manso Sanchez, L.; Xu, B.; Luu, T.; Dieras, V.; Hershman, D. L.; Agrapart, V.; Ananthakrishnan, R.; Staroslawska, E. Safety and Efficacy of Neratinib (HKI-272) plus Vinorelbine in the Treatment of Patients with ErbB2-Positive Metastatic Breast Cancer Pretreated with Anti-HER2 Therapy. *Ann. Oncol.* **2013**, *24* (1), 109−116.

(7) Owens, M. A.; Horten, B. C.; Da Silva, M. M. HER2 Amplification Ratios by Fluorescence in Situ Hybridization and Correlation with Immunohistochemistry in a Cohort of 6556 Breast Cancer Tissues. *Clin. Breast Cancer* **2004**, *5*, 63−69.

(8) Qian, Z. M. Targeted Drug Delivery via the Transferrin Receptor-Mediated Endocytosis Pathway. *Pharmacol. Rev.* **2002**, *54*, 561−587.

(9) Zhu, Z. Targeted Cancer Therapies Based on Antibodies Directed against Epidermal Growth Factor Receptor: Status and Perspectives. *Acta Pharmacol. Sin.* **2007**, *28*, 1476−1493.

(10) Müller, A.; Homey, B.; Soto, H.; Ge, N.; Catron, D.; Buchanan, M. E.; McClanahan, T.; Murphy, E.; Yuan, W.; Wagner, S. N.; Barrera, J. L.; Mohar, A.; Verástegui, E.; Zlotnik, A. Involvement of Chemokine Receptors in Breast Cancer Metastasis. *Nature* **2001**, *410*, 50−56.

(11) Wu, B.; Chien, E. Y. T.; Mol, C. D.; Fenalti, G.; Liu, W.; Katritch, V.; Abagyan, R.; Brooun, A.; Wells, P.; Bi, F. C.; Hamel, D. J.; Kuhn, P.; Handel, T. M.; Cherezov, V.; Stevens, R. C. Structures of the CXCR4 Chemokine GPCR with Small-Molecule and Cyclic Peptide Antagonists. *Science* **2010**, *330*, 1066−1071.

(12) Busillo, J. M.; Benovic, J. L. Regulation of CXCR4 Signaling. *Biochim. Biophys. Acta, Biomembr.* **2007**, *1768*, 952−963.

(13) Yang, J.; Moses, M. A. Lipocalin 2: A Multifaceted Modulator of Human Cancer. *Cell Cycle* **2009**, *8*, 2347−2352.

(14) Bauer, M.; Eickhoff, J. C.; Gould, M. N.; Mundhenke, C.; Maass, N.; Friedl, A. Neutrophil Gelatinase-Associated Lipocalin (NGAL) Is a Predictor of Poor Prognosis in Human Primary Breast Cancer. *Breast Cancer Res. Treat.* **2008**, *108*, 389−397.

(15) Yang, J.; Bielenberg, D. R.; Rodig, S. J.; Doiron, R.; Clifton, M. C.; Kung, A. L.; Strong, R. K.; Zurakowski, D.; Moses, M. A. Lipocalin 2 Promotes Breast Cancer Progression. *Proc. Natl. Acad. Sci. U.S.A.* **2009**, *106*, 3913−3918.

(16) Leng, X.; Ding, T.; Lin, H.; Wang, Y.; Hu, L.; Hu, J.; Feig, B.; Zhang, W.; Pusztai, L.; Symmans, W. F.; Wu, Y.; Arlinghaus, R. B. Inhibition of Lipocalin 2 Impairs Breast Tumorigenesis and Metastasis. *Cancer Res.* **2009**, *69*, 8579−8584.

(17) Scherr, M.; Battmer, K.; Schultheis, B.; Ganser, A.; Eder, M. Stable RNA Interference (RNAi) as an Option for Anti-Bcr-Abl Therapy. *Gene Ther.* **2005**, *12*, 12−21.

(18) Morrissey, D. V.; Lockridge, J. A.; Shaw, L.; Blanchard, K.; Jensen, K.; Breen, W.; Hartsough, K.; Machemer, L.; Radka, S.; Jadhav, V.; Vaish, N.; Zinnen, S.; Vargeese, C.; Bowman, K.; Shaffer, C. S.; Jeffs, L. B.; Judge, A.; MacLachlan, I.; Polisky, B. Potent and Persistent in Vivo Anti-HBV Activity of Chemically Modified siRNAs. *Nat. Biotechnol.* **2005**, *23*, 1002−1007.

(19) Landen, C. N.; Chavez-Reyes, A.; Bucana, C.; Schmandt, R.; Deavers, M. T.; Lopez-Berestein, G.; Sood, A. K. Therapeutic EphA2 Gene Targeting in Vivo Using Neutral Liposomal Small Interfering RNA Delivery. *Cancer Res.* **2005**, *65*, 6910−6918.

(20) Soutschek, J.; Akinc, A.; Bramlage, B.; Charisse, K.; Constien, R.; Donoghue, M.; Elbashir, S.; Geick, A.; Hadwiger, P.; Harborth, J.; John, M.; Kesavan, V.; Lavine, G.; Pandey, R. K.; Racie, T.; Rajeev, K. G.; Röhl, I.; Toudjarska, I.; Wang, G.; Wuschko, S.; Bumcrot, D.; Koteliansky, V.; Limmer, S.; Manoharan, M.; Vornlocher, H.-P. Therapeutic Silencing of an Endogenous Gene by Systemic Administration of Modified siRNAs. *Nature* **2004**, *432*, 173−178.

(21) Zhang, M.; Zhou, Y.; Xie, C.; Zhou, F.; Chen, Y.; Han, G.; Zhang, W. J. STAT6 Specific shRNA Inhibits Proliferation and Induces Apoptosis in Colon Cancer HT-29 Cells. *Cancer Lett.* **2006**, *243*, 38−46.

(22) Gómez-Valadés, A. G.; Vidal-Alabró, A.; Molas, M.; Boada, J.; Bermúdez, J.; Bartrons, R.; Perales, J. C. Overcoming Diabetes-Induced Hyperglycemia through Inhibition of Hepatic Phosphoenolpyruvate Carboxykinase (GTP) with RNAi. *Mol. Ther.* **2006**, *13*, 401−410.

(23) Scherr, M.; Battmer, K.; Schultheis, B.; Ganser, A.; Eder, M. Stable RNA Interference (RNAi) as an Option for Anti-Bcr-Abl Therapy. *Gene Ther.* **2005**, *12*, 12−21.

(24) Gonzalez-Alegre, P.; Bode, N.; Davidson, B. L.; Paulson, H. L. Silencing Primary Dystonia: Lentiviral-Mediated RNA Interference Therapy for DYT1 Dystonia. *J. Neurosci.* **2005**, *25*, 10502−10509.

(25) Mok, H. P.; Lever, A. M. L. Vector Integration: Location, Location, Location. *Gene Ther.* **2005**, *12*, 1−2.

(26) Taulli, R.; Accornero, P.; Follenzi, A.; Mangano, T.; Morotti, A.; Scuoppo, C.; Forni, P. E.; Bersani, F.; Crepaldi, T.; Chiarle, R.; Naldini, L.; Ponzetto, C. RNAi Technology and Lentiviral Delivery as a Powerful Tool to Suppress Tpr-Met-Mediated Tumorigenesis. *Cancer Gene Ther.* **2005**, *12*, 456−463.

(27) Rubinson, D. A.; Dillon, C. P.; Kwiatkowski, A. V.; Sievers, C.; Yang, L.; Kopinja, J.; Rooney, D. L.; Zhang, M.; Ihrig, M. M.; McManus, M. T.; Gertler, F. B.; Scott, M. L.; Van Parijs, L. A Lentivirus-Based System to Functionally Silence Genes in Primary Mammalian Cells, Stem Cells and Transgenic Mice by RNA Interference. *Nat. Genet.* **2003**, *33*, 401−406.

(28) Zhang, C.; Tang, N.; Liu, X.; Liang, W.; Xu, W.; Torchilin, V. P. siRNA-Containing Liposomes Modified with Polyarginine Effectively Silence the Targeted Gene. *J. Controlled Release* **2006**, *112*, 229−239.

(29) Auguste, D.; Furman, K.; Wong, A.; Fuller, J.; Armes, S.; Deming, T.; Langer, R. Triggered Release of siRNA from Poly-(ethylene Glycol)-Protected, pH-Dependent Liposomes. *J. Controlled Release* **2008**, *130*, 266−274.

(30) Epstein, R. J. The CXCL12-CXCR4 Chemotactic Pathway as a Target of Adjuvant Breast Cancer Therapies. *Nat. Rev. Cancer* **2004**, *4*, 901−909.

(31) Salvucci, O.; Bouchard, A.; Baccarelli, A.; Deschenes, J.; Sauter, G.; Simon, R.; Bianchi, R.; Basik, M. The Role of CXCR4 Receptor Expression in Breast Cancer: A Large Tissue Microarray Study. *Breast Cancer Res. Treat.* **2005**, *97*, 275−283.
(32) Gunawan, R. C.; Auguste, D. T. The Role of Antibody Synergy and Membrane Fluidity in the Vascular Targeting of Immunoliposomes. *Biomaterials* **2010**, *31*, 900−907.
(33) Uhlen, M.; Oksvold, P.; Fagerberg, L.; Lundberg, E.; Jonasson, K.; Forsberg, M.; Zwahlen, M.; Kampf, C.; Wester, K.; Hober, S.; Wernerus, H.; Björling, L.; Ponten, F. Towards a Knowledge-Based Human Protein Atlas. *Nat. Biotechnol.* **2010**, *28*, 1248−1250.
(34) Uhlen, M. A Human Protein Atlas for Normal and Cancer Tissues Based on Antibody Proteomics. *Mol. Cell. Proteomics* **2005**, *4*, 1920−1932.
(35) Pontén, F.; Jirström, K.; Uhlen, M. The Human Protein Atlas-a Tool for Pathology. *J. Pathol.* **2008**, *216*, 387−393.
(36) Lundberg, E.; Fagerberg, L.; Klevebring, D.; Matic, I.; Geiger, T.; Cox, J.; Älgenäs, C.; Lundeberg, J.; Mann, M.; Uhlen, M. Defining the Transcriptome and Proteome in Three Functionally Different Human Cell Lines. *Mol. Syst. Biol.* **2010**, DOI: 10.1038/msb.2010.106.
(37) Pontén, F.; Gry, M.; Fagerberg, L.; Lundberg, E.; Asplund, A.; Berglund, L.; Oksvold, P.; Björling, E.; Hober, S.; Kampf, C.; Navani, S.; Nilsson, P.; Ottosson, J.; Persson, A.; Wernérus, H.; Wester, K.; Uhlén, M. A Global View of Protein Expression in Human Cells, Tissues, and Organs. *Mol. Syst. Biol.* **2009**, 10.1038/msb.2009.93.
(38) Guo, P.; You, J.-O.; Yang, J.; Moses, M. A.; Auguste, D. T. Using Breast Cancer Cell CXCR4 Surface Expression to Predict Liposome Binding and Cytotoxicity. *Biomaterials* **2012**, *33*, 8104−8110.
(39) Semple, S. C.; Klimuk, S. K.; Harasym, T. O.; Dos Santos, N.; Ansell, S. M.; Wong, K. F.; Maurer, N.; Stark, H.; Cullis, P. R.; Hope, M. J.; Scherrer, P. Efficient Encapsulation of Antisense Oligonucleotides in Lipid Vesicles Using Ionizable Aminolipids: Formation of Novel Small Multilamellar Vesicle Structures. *Biochim. Biophys. Acta* **2001**, *1510*, 152−166.
(40) You, J.-O.; Almeda, D.; Ye, G. J.; Auguste, D. T. Bioresponsive Matrices in Drug Delivery. *J. Biol. Eng.* **2010**, *4*, 15.
(41) Hillaireau, H.; Couvreur, P. Nanocarriers' Entry into the Cell: Relevance to Drug Delivery. *Cell. Mol. Life Sci.* **2009**, *66*, 2873−2896.
(42) Jølck, R. I.; Feldborg, L. N.; Andersen, S.; Moghimi, S. M.; Andresen, T. L. Engineering Liposomes and Nanoparticles for Biological Targeting. In *Biofunctionalization of Polymers and their Applications*; Nyanhongo, G. S., Steiner, W., Gübitz, G., Eds.; Springer Berlin Heidelberg: Berlin, Heidelberg, 2010, Vol. *125*; pp 251−280.
(43) Son, K. K.; Patel, D. H.; Tkach, D.; Park, A. Cationic Liposome and Plasmid DNA Complexes Formed in Serum-Free Medium under Optimum Transfection Condition Are Negatively Charged. *Biochim. Biophys. Acta* **2000**, *1466*, 11−15.
(44) Rhodes, L. V.; Bratton, M. R.; Zhu, Y.; Tilghman, S. L.; Muir, S. E.; Salvo, V. A.; Tate, C. R.; Elliott, S.; Nephew, K. P.; Collins-Burow, B. M.; Burow, M. E. Effects of SDF-1-CXCR4 Signaling on microRNA Expression and Tumorigenesis in Estrogen Receptor-Alpha (ER-A)-Positive Breast Cancer Cells. *Exp. Cell Res.* **2011**, *317*, 2573−2581.
(45) Wang, J.; Cai, J.; Han, F.; Yang, C.; Tong, Q.; Cao, T.; Wu, L.; Wang, Z. Silencing of CXCR4 Blocks Progression of Ovarian Cancer and Depresses Canonical Wnt Signaling Pathway. *Int. J. Gynecol. Cancer* **2011**, *21*, 981−987.
(46) Wang, Z.; Ma, Q.; Liu, Q.; Yu, H.; Zhao, L.; Shen, S.; Yao, J. Blockade of SDF-1/CXCR4 Signalling Inhibits Pancreatic Cancer Progression in Vitro via Inactivation of Canonical Wnt Pathway. *Br. J. Cancer* **2008**, *99*, 1695−1703.
(47) Shi, H.; Gu, Y.; Yang, J.; Xu, L.; Mi, W.; Yu, W. Lipocalin 2 Promotes Lung Metastasis of Murine Breast Cancer Cells. *J. Exp. Clin. Cancer Res.* **2008**, *27*, 83.
(48) Teicher, B. A.; Fricker, S. P. CXCL12 (SDF-1)/CXCR4 Pathway in Cancer. *Clin. Cancer Res.* **2010**, *16*, 2927−2931.